

# We are IntechOpen, the world's leading publisher of Open Access books Built by scientists, for scientists

6,900

Open access books available

185,000

International authors and editors

200M

Downloads

Our authors are among the

154

Countries delivered to

TOP 1%

most cited scientists

12.2%

Contributors from top 500 universities



WEB OF SCIENCE™

Selection of our books indexed in the Book Citation Index  
in Web of Science™ Core Collection (BKCI)

Interested in publishing with us?  
Contact [book.department@intechopen.com](mailto:book.department@intechopen.com)

Numbers displayed above are based on latest data collected.  
For more information visit [www.intechopen.com](http://www.intechopen.com)



---

# Novel Biopolymer Composite Membrane Involved with Selective Mass Transfer and Excellent Water Permeability

---

Peng Wu and Masanao Imai

Additional information is available at the end of the chapter

<http://dx.doi.org/10.5772/50697>

---

## 1. Introduction

Applications of bio-polymeric materials have increased significantly for both textile engineering and medical sciences. Use of biopolymer in place of artificial polymers has been increasing due to stringent environmental regulations [1]. The development of new-generation materials that extend the industrial and biomedical applications of membrane processes will require a high level of control of the characteristics of the base polymeric support layer [2]. Current research in membrane science is now focusing more on biopolymers from natural raw material with well-defined structure to develop new membrane materials [3]. Noticeably, biopolymer production can be sustainable, carbon neutral, and renewable because biopolymers are made from sea or land plant materials that can be grown year after year indefinitely. Novel biopolymer membranes enable separation based on other driving forces like electrical charge and physicochemical interactions, and with appropriate functional groups can provide applications such as tunable water permeation and separation, toxic metal capture, toxic organic dechlorination, and biocatalysts [4-5].

Biopolymers for stabilizers, thickeners, and gelling agents were extracted from various raw natural resources. They determine a number of critical functions including moisture binding, control, structure, and flow behavior that enable organisms to thrive in a natural environment [6]. A number of the typical biopolymers from natural resources such as alginate, cellulose, and chitin/chitosan have been applied for functional polymer networks (e.g., carriers for controlled drug release, membranes with regulated permeability, sensor devices, and artificial muscles). For these purposes, proper responses to changes in external physicochem-

ical conditions and developed internal microstructure of the gels are required. Interest in the behavior of biopolymer gels and networks has grown significantly. The various hydrophilic bio and/or artificial polymers that can be used for membrane formation are also discussed.

Various novel membrane materials and systems have been developed and applied. The technological benefits of such membrane materials and systems have begun to be identified for a wide range of applications for controlled drug delivery, chemical separation, water treatment, bio-separation, chemical sensors, tissue engineering, etc. There have been two main subjects of research in the field of biopolymer membrane materials and systems: development of novel and efficient biopolymer materials and improvement of capability of membrane processes and operations [7].

This chapter discusses the novel function of polysaccharides ( $\kappa$ -carrageenan ( $\kappa$ C) and pullulan (P)) in membrane formation and molecular-size screening. The  $\kappa$ -carrageenan mass fraction ( $F_C$ ) was a key factor in determining membrane characteristics for both selected molecular permeability and mechanical strength.

## 2. Development of Biopolymer membranes

When discussing biopolymer gelation, the biopolymer types of interest fall naturally into two categories: protein and polysaccharides. A second classification is in terms of the molecular networks underlying the gels, that is, in terms of associative and particulate networks [8]. The present status of biological and ecological research demands much more emphasis on efficient biopolymers with multiple applications such as membrane-separation engineering.

One of the most common membrane types currently in use is the asymmetric cellulose acetate (CA) membrane. This high-flux, high-rejection membrane was developed in the early 1960s by Loeb and Sourirajan [9]. Chitin, poly ( $\beta$ -(1-4)-N-acetyl-D-glucosamine), is a natural polysaccharide of major importance, first identified in 1884. When the degree of deacetylation of chitin reaches about 50% (depending on the origin of polymer), it becomes soluble in aqueous acidic media and is called chitosan [10-11]. Chitosan membranes have been explored in many uses, such as in water-ethanol pervaporation [12-14], enzyme immobilization and cationic specimen transportation [15-16], protein separation [17] and concentration, controlled ingredient-release, and environmental applications [18-19]. Among the various biopolymers, alginate is the most studied matrix for membrane separation technology [20]. Hirst and Rees (1965) were the first to postulate that alginate is a polymer of mannuronic acid and guluronic acid having 1,4 linkage. Kashima and Imai (2011) investigated the  $\alpha$ -L-guluronic acid chain with regard to regulation of the mass-transfer characteristics of the alginate membrane [21]. Many other biopolymers also consist of membrane structures. Exploiting and improving the chemical and mechanical properties of biopolymer membranes will create many more applications in the membrane industry.

### 3. Novel biopolymer membrane materials ( $\kappa$ -carrageenan & pullulan)

Biopolymers of marine algae origin are ubiquitous in surface waters and have attractive potential. The seaweed extractives of commercial importance fall into three main groups, two of which (agar and carrageenans) are derived from red algae, and the third (alginates) from brown algae. All three types of extractive are associated with the cell walls of the algae and resemble cellulose in basic molecular organization. Red algae are considered as the most important resource of many biologically active metabolites compared to other algal classes [22-23]. Marine algae as carrageenans have optimum growth conditions with sufficient sun light, stable temperature, and no climate change impact on the ground; stable harvests are thus expected. Marine algae can be produced in virtually unlimited amounts around seafaring nations. It contributes noticeably on the preventing Global Warming and coexistent with fishery.

Carrageenans are large, highly flexible molecules that curl and form helical structures. They are widely used in food and other industries as thickening and stabilizing agents. Carrageenans consist of alternating copolymers of  $\alpha$ -(1 $\rightarrow$ 3)-D-galactose and  $\beta$ -(1 $\rightarrow$ 4)-3,6-anhydro-D- or L-galactose. Several isomers of carrageenan are known ( $\kappa$ -,  $\iota$ -, and  $\lambda$ -carrageenans), and they differ in the number and position of the ester sulfate groups on the repeating galactose units.  $\kappa$ -Carrageenan has only one negative charge per disaccharide and tends to form a strong and rigid gel. The gelling power of  $\kappa$ -carrageenans imparts excellent film-forming properties, and  $\kappa$ -carrageenan forms a firm gel with the aid of potassium ions. Hot solutions of  $\kappa$ -carrageenans set when cooled below the gel point, which is between 30° and 70°, depending on the cations and other ingredients present, to form a range of gel textures. The two-step gel mechanism is illustrated in Fig. 1, with stage B being elastic (iota) and stage C being brittle (kappa).

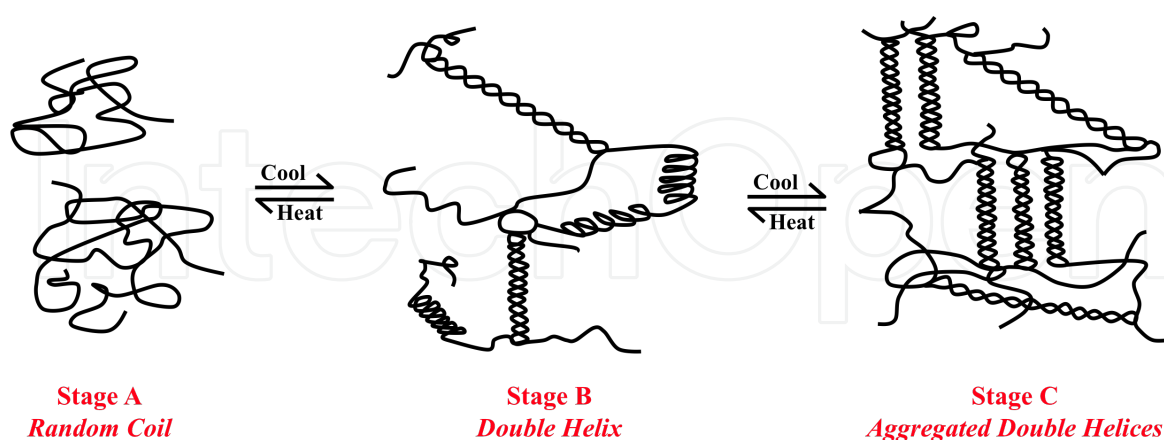


**Figure 1.** Models of conformational transition of  $\kappa$ -carrageenan and  $\iota$ -carrageenan.

$\kappa$ -Carrageenan selects potassium ions to stabilize the junction zones within the characteristically firm, brittle gel. Potassium ions counter sulphate charges without sterically hindering close approach and double-helix formation (Fig. 2) [24-30].

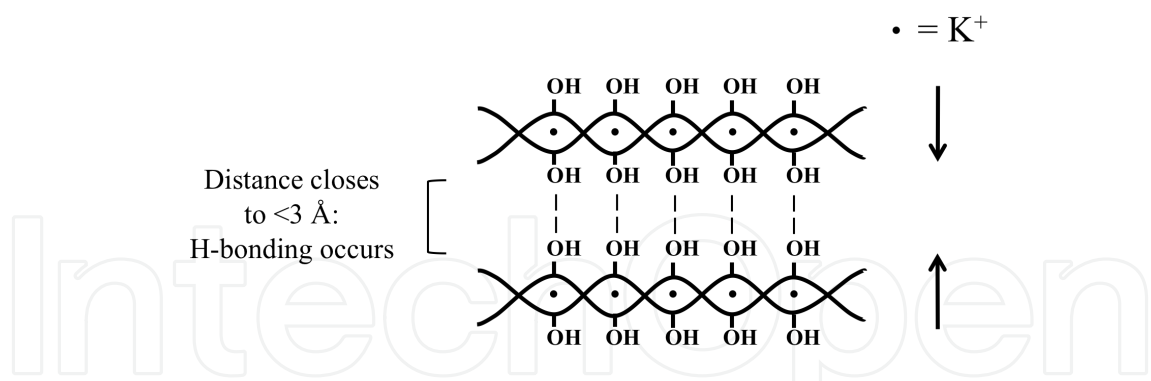


**Figure 2.** The gelation mechanism of  $\kappa$ -Carrageenan crosslinked by  $\text{K}^+$  ions.

Pullulan is an extracellular glucan elaborated by a fungus of the genus *Aureobasidium*, commonly called black yeast. The structure of pullulan is a linear glucan consisting of repeating units of maltotriose joined by  $\alpha$ -D-(1 $\rightarrow$ 6) linkages. The safety of pullulan in foods is supported by its chemical composition, the purity of the final product, a series of toxicological studies, and the fact that it has been used about 30 years as an ingredient in human foods in Japan [31-33]. Recently, the demand for pullulan has rapidly increased for films and hard capsules, and its use in these fields is expected to grow [34-35]. The major interest in pullulan concerns its capacity to form strong, resilient films and fibers [36]. Pullulan can be used on its own or combined with other thickeners or gelling agents. The stringiness of pullulan may be a disadvantage for some applications, but this can be modified by adding a small amount of another polysaccharide such as carrageenan or xanthan gum [37]. Combinations of  $\kappa$ -carrageenan and pullulan achieve gel-network strengths and elasticity between the two extremes and consistent with the ratio used (Fig. 3).

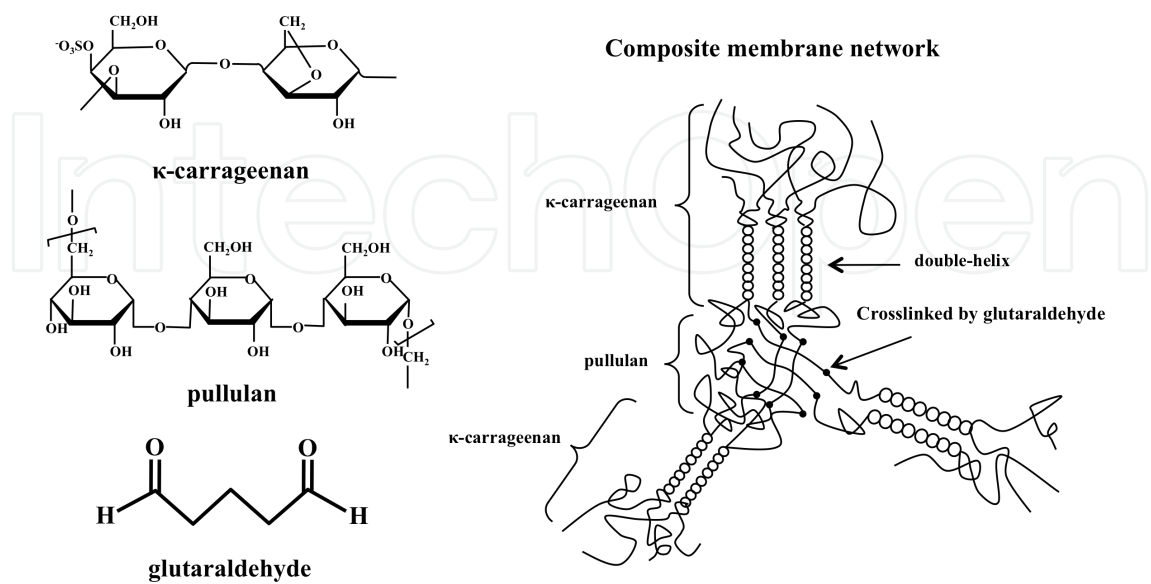


**Figure 3.** Schematic representation of composite  $\kappa$ -carrageenan-pullulan chains.

In our study, original biopolymer composite membrane was successfully prepared from marine biopolymer ( $\kappa$ -carrageenan) and food polysaccharide (pullulan). Selective mass transfer and excellent water permeability were achieved. The membrane was characterized from the mass fraction of  $\kappa$ -carrageenan. The attractive potential of marine biopolymer ( $\kappa$ -carrageenan) combined with polysaccharide (pullulan) was demonstrated in membrane-separation engineering. The authors focused on the complex cross-linked biopolymers ( $\kappa$ -carrageenan and pullulan) regulating mass-transfer flux. The membrane was prepared by a simple casting method. The  $\kappa$ -carrageenan-pullulan composite membrane has sufficient mechanical strength for practical use and excellent mass-transfer characteristics, especially for molecular-size screening.

#### 4. Polymer membranes preparation

The most important part in any membrane separation process is choosing the membrane material. Membranes have very different structures, functions, transport properties, transport mechanisms, and materials. The methods of making membranes are just as diverse as the membranes are. The methods of making membranes are considering the large diversity suited for technical application. The following characteristic of membranes determine separation capability.

- Membrane materials.

Organic polymers, inorganic materials (oxides, ceramics, and metals), or composite materials.

- Membrane cross-section.

Isotropic (symmetric), integrally anisotropic (asymmetric), bi- or multilayer, thin-layer or mixed matrix composites.

- Preparation methods.

Phase separation (phase inversion) of polymers, sol-gel process, interface reaction, stretching, extrusion, track-etching, and micro-fabrication.

- Membrane shape.

Sheet, hollow fiber, capsule.

The process for forming a biopolymer membrane comprises three steps.:

I. Mixing a biomaterial in a solvent to define a gel.

II. Drying the gel to define a sponge having a solvent content.

III. Adjusting the solvent content of the sponge so that the sponge is substantially filled with the solvent.



4.1. Preparing of κ-carrageenan/pullulan composite membranes

κ-Carrageenan and pullulan powders were dissolved in distilled water (70°C) using a magnetic stirrer to prepare film-forming solutions of various blend-weight ratios. All polymer solutions were prepared based on 3g total polymer weight dissolved in 97g of distilled water at 70°C for one hour. In addition, each solution was stirred for one hour at 70°C. Glutaraldehyde solution (30 ~ 130mM) was introduced into the polymer solutions [39]. And then twenty grams of the polymer solutions was then cast into a petri dish, followed by drying in an electrical blast-drying chest at 65°C for 24 hours. The dried membranes (attached to the petri dishes) were immersed in potassium chloride solution [40] (0.1 to 1.0M) for 24 hours. The swollen membrane spontaneously peeled from the petri dish at 25 ± 1°C and was washed clean with pure water for further testing. Membrane samples were tested in triplicate. Pure pullulan single component membrane (cross-linked by glutaraldehyde) was too weak to make a flat membrane in our study [41].

Mass fraction of κ-carrageenan ( $F_c$ )	$F_c$ [-]	κ-carrageenan [g]	Pullulan [g]
$F_c = \frac{\kappa - carrageenan[g]}{\kappa - carrageenan[g] + pullulan[g]}$	0.33	1.00	2.00
	0.42	1.25	1.75
	0.5	1.50	1.50
	0.58	1.75	1.25
	0.66	2.00	1.00
	0.75	2.25	0.75

Table 1. Mass fraction of κ-carrageenan ( $F_c$ ).

5. Measurement of biopolymer composite membranes’ properties

Commercial membrane applications focus much effort on desalination requirements [42-43], membrane-fouling characterization [44-45], drinking-water disinfection [46-47], industrial waste treatment [48-49], food industry material separation [50-51], adsorption desalination [52-53], biofiltration [54], membrane bioreactor [55-56], thermal distillation [57], electrodialysis desalination [58], reverse-osmosis desalination [59], oil-water separation applications [60], and future membrane and desalination developments. The stress-strain correlation of biopolymer membrane is affected by the origin of polymers, molecular weight, and methods of membrane preparation, conditioning, and cross-linking. Biopolymer membranes may be amorphous homopolymers or heterogeneous, depending on whether they are prepared from a single polymer or from blended polymers [61]. However, the properties of biopolymer membranes are inconsistent with the requirements of industrial-processing technologies, since the range of biopolymers suitable for membrane-separation processes is limited. To expand the application area of commercial membranes, research on improving their properties is necessary.

### 5.1. Mechanical properties of $\kappa$ -carrageenan/pullulan composite membrane

A rheometer (CR-DX500, Sun Scientific Co., Ltd., Tokyo, Japan) was used to determine the tensile strength and the percentage elongation at break. Three rectangular-strip specimens (10mm wide, 40mm long) were cut from each membrane for tensile testing. The initial grip separation was set to 20mm, and the crosshead speed was set to 1mm/s. The initial membrane thickness was measured using a micrometer (Mitutoyo, Kanagawa, Japan). The average thickness of the membrane strip was used to estimate the initial cross-sectional area of the membrane sample. Maximum Stress ( $\sigma$ ) (MPa) was calculated by dividing the maximum load (N) by the initial cross-sectional area (m<sup>2</sup>):

$$\sigma = \frac{T}{(b \times d)} \quad (1)$$

where  $T$  is the maximum load (N),  $b$  is the width of sample (m), and  $d$  is the membrane thickness (m).

Maximum Strain ( $\lambda$ ) (%) was calculated as follows:

$$\lambda = \frac{(L - L_0)}{(L_0)} \times 100\% \quad (2)$$

where  $L_0$  is the sample length before deformation and  $L$  is the sample length at break [62].

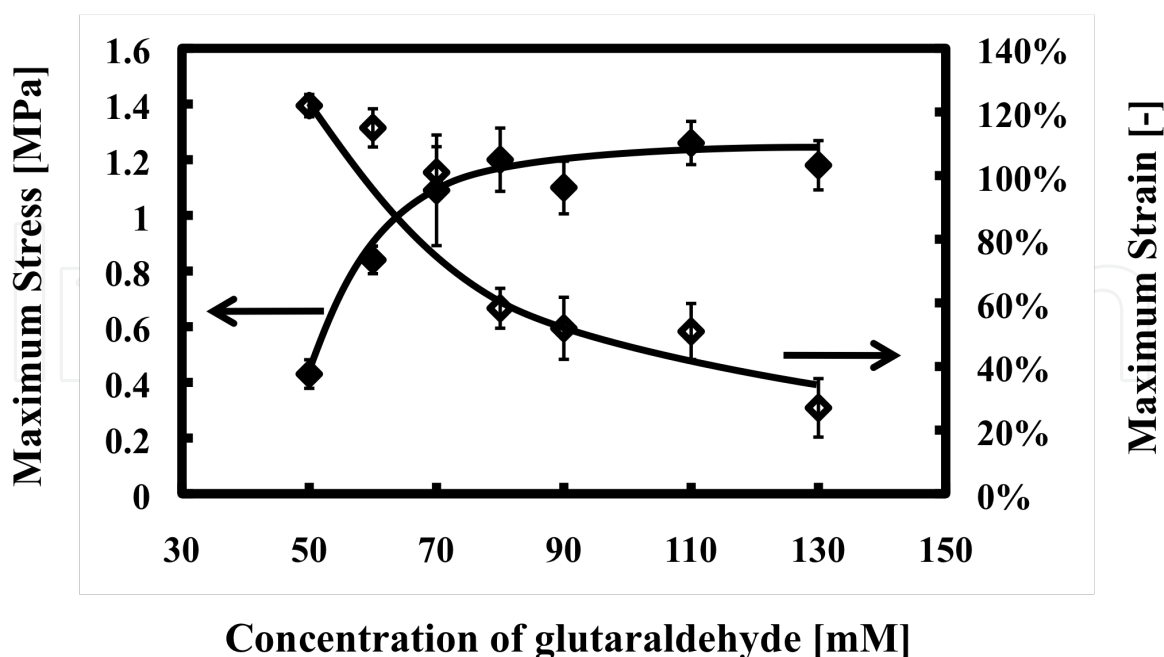


**Figure 4.** Effect of additive glutaraldehyde concentration on the maximum stress and strain of composite membrane.  $F_c$  was set at 0.33.



Dehydration of hydroxyl groups in the polysaccharide chain by glutaraldehyde facilitates formation of polymer networks. The polysaccharide composite membrane was further cross-linked with glutaraldehyde to reduce swelling and increase the structural strength of the membrane as well as to improve its thermal and mechanical stability [63]. The lower  $F_C$  membrane is convenient for investigating the influence of dehydration by glutaraldehyde because the lower  $F_C$  membrane contains many hydroxyl groups bonding to pullulan. The mechanical stress increased with increasing concentration of glutaraldehyde and became constant over 70mM. Figure 4 presents the polymeric framework of the membrane densely populated with increasing glutaraldehyde concentration.

$F_C$  0.75 membrane accounts for the largest mass fraction of  $\kappa$ -carrageenan.  $\kappa$ -carrageenan is a key component for constructing the gel structure and for characterizing mechanical strength.

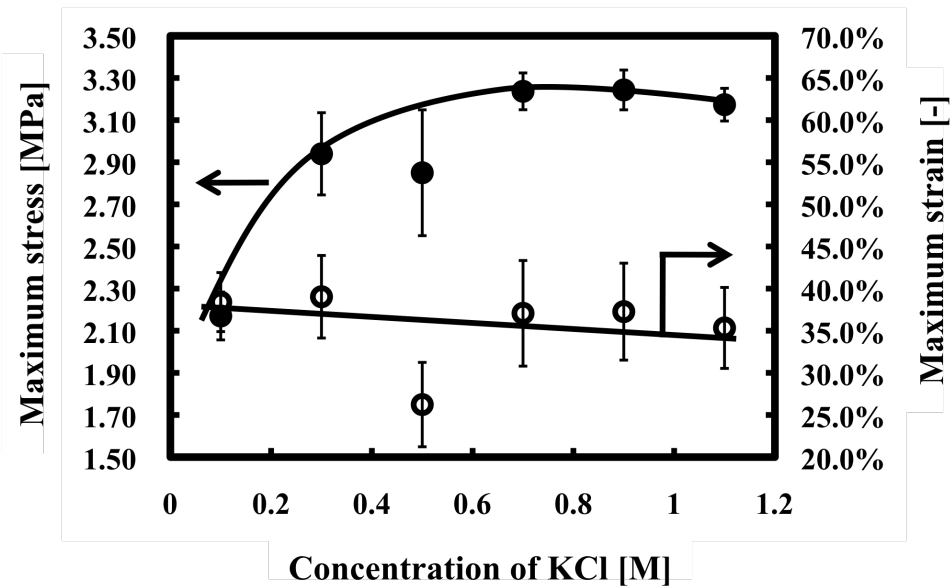


**Figure 5.** Effect of potassium chloride-immersion on the maximum stress and the strain of composite membrane.  $F_C$  was set at 0.75.

The authors prepared  $\kappa$ -carrageenan/pullulan membranes with 90mM of glutaraldehyde added and 0.7M potassium chloride-immersion. (Fig. 5)

5.2. Water content

Water content is important for evaluating hydrophilic characteristics. The volumetric water content of the membrane indicated voids in the network that affect the water permeability [64]. Gravimetric methods were used to determine the mass-based water content ( $W_t$ ) [65]. The water content ( $W_t$ ) was measured as follows. Membranes were immersed in distilled water at  $25\pm1^\circ\text{C}$  for 1 day to achieve natural hydration and swelling. The membranes were removed from the water bath, and excess water on the membrane surface was removed by filter paper. The mass of the swollen membrane  $W_w$  was then determined.

$$W_t = \frac{(W_w - W_d)}{W_w} \times 100\% \quad (3)$$

Here,  $W_d$  is the mass of the dried membrane.

### 5.3. Scanning Electron Microscopy (SEM)

The membranes were snap-frozen in liquid nitrogen then dried in a vacuum freeze dryer (RLE-103, Kyowa Vacuum Engineering. Co., Ltd., Tokyo, Japan) (298 K) for 24 hours. The membranes were then sputter-coated with a thin film of Pt, using a sputter-coater (E-1010 Ion Sputter, Hitachi, Ltd., Tokyo, Japan). Images of cross sections of the membranes were obtained using a scanning electron microscope (Miniscope TM-1000, Hitachi, Ltd.,).

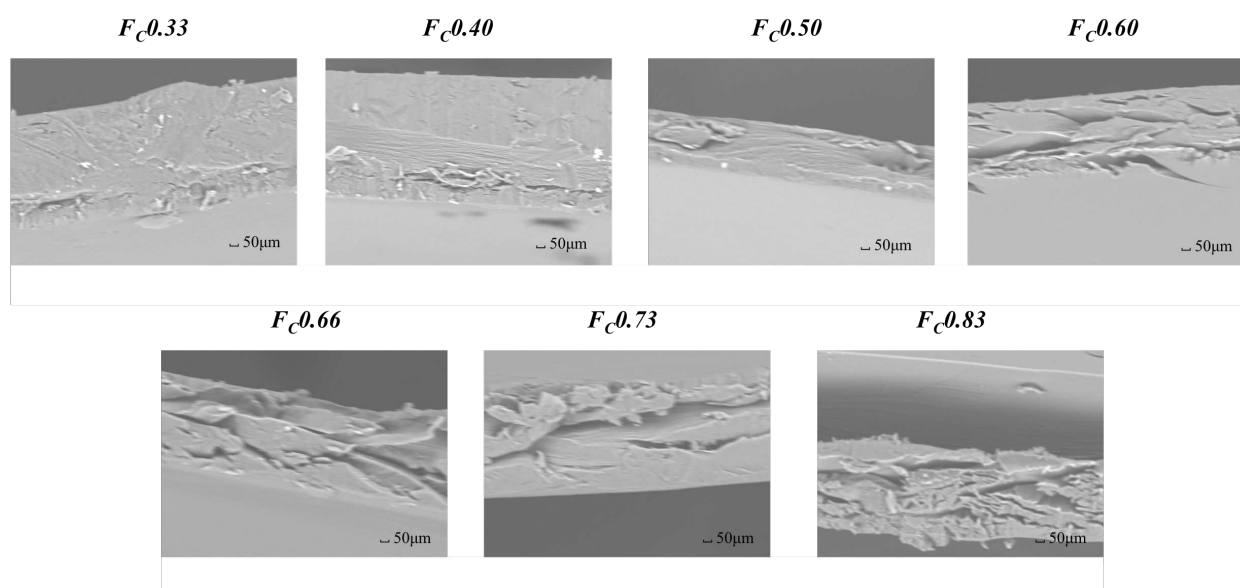


**Figure 6.** SEM images of  $\kappa$ -carrageenan/pullulan composite membrane.

## 6. Mass transfer in biopolymer membrane

The prolific application of membrane separation processes in industry today is primarily due to innovations in membrane materials technology. Loeb and Sourirajan (1963) pioneered the first reverse-osmosis (RO) asymmetric cellulose acetate (CA) membrane capable of withstanding the rigors of industrial use [66]. Since then, many types of biopolymer membranes have been developed and commercialized: membranes for microfiltration (MF) [67-68], ultrafiltration (UF) [69-70], nanofiltration (NF) [71-72], gas separation [73-74], and so on. These membrane separation systems are illustrated in Fig. 7.

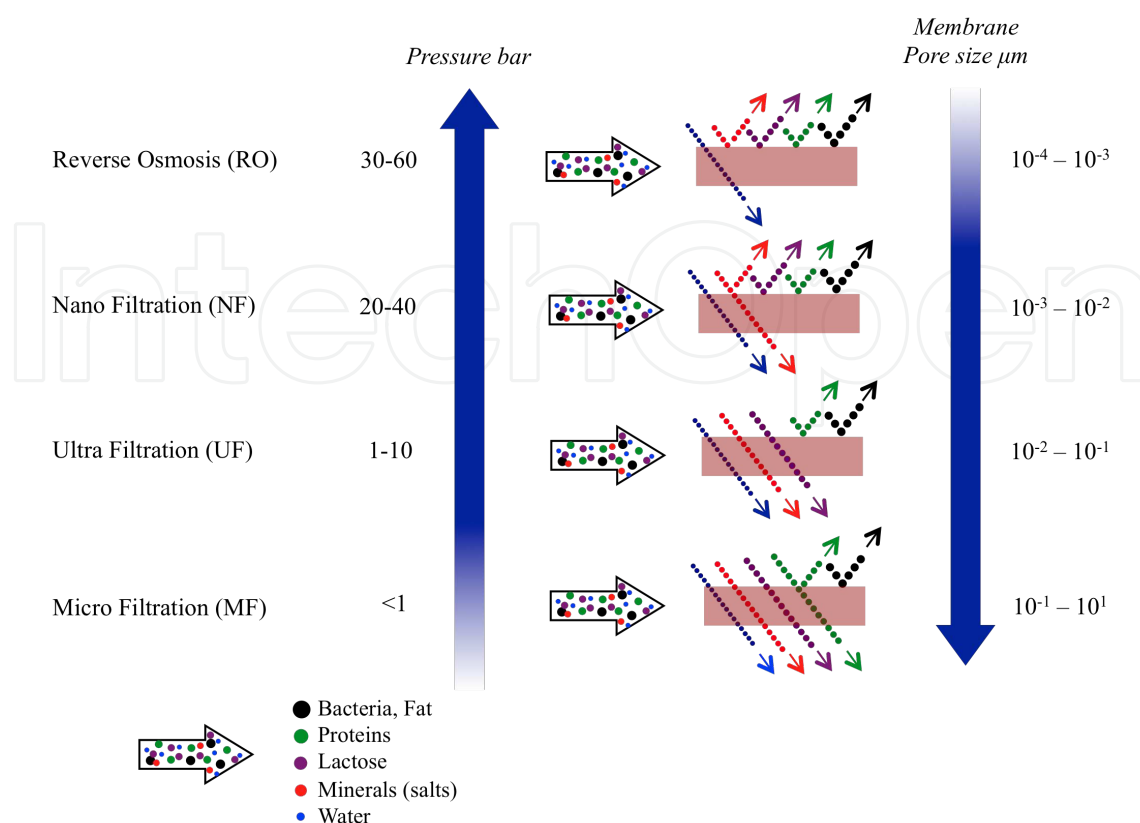


**Figure 7.** Principles of membrane filtration.

The energy consumption for these technological filtration (MF, UF, and NF) processes is low, as latent heat in the phase change is not consumed in the membrane separation process. Membrane separation is expected to be one of the most promising and energy-efficient separation technologies. Diffusion of solutes through non-porous biopolymer membranes is discussed using a molecular-diffusion model [75-76].

In many conventional porous membranes, the membrane material is not an active participant; only its pore structure matters, not its chemical structure [77]. A common feature of biopolymer membranes in the solution-diffusion process is that the solute molecules dissolved in the biopolymer membranes diffuse through the polymer chains (also called mass-transfer channels) and then exit the membrane at the other side phase [78]. The biopolymer is an active participant in both the solution and diffusion processes.

### 6.1. Diffusion in biopolymer membrane

According to a solution-diffusion mechanism based on Fick's law (Eq. 4) [79], mass transfer flux was indicated as followed:

$$J_i = -D \frac{dc_i}{dx} \quad (4)$$

where

$J_i$  is the flux of component  $i$  ( $\text{mol}/(\text{m}^2\text{s})$ ),

$D$  is the diffusion coefficient ( $\text{m}^2/\text{s}$ ), and

$dc_i/dx$  is the concentration gradient for component  $i$  over the length  $x$  ( $\text{mol}/(\text{m}^3\text{m})$ ).

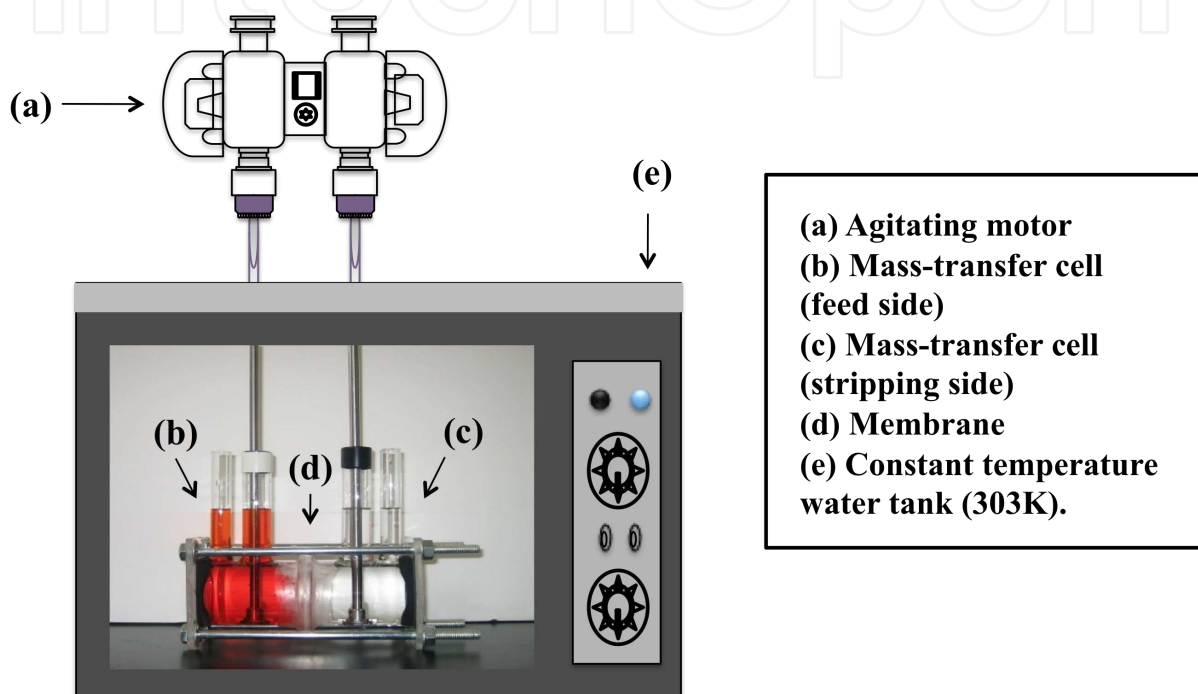


**Figure 8.** Schematic diagram of the mass-transfer setup in our experiment.

In this chapter, mass-transfer experiments were carried out using a standard side-by-side diffusion cell with two compartments separated by a membrane with an area of  $23\text{cm}^2$  (Fig. 8).

The diffusion cell was installed in a water bath to keep the temperature constant ( $303\text{K}$ ). The feed compartment was filled with water-soluble marker components in solution ( $190\text{ml}$ ) (Fig. 9), and the stripping compartment was filled with distilled water. During the experiment, the two compartments of solutions were stirred at a constant speed ( $850\text{min}^{-1}$ ) in order to minimize the film mass-transfer resistance near the membrane surface. The solutions in the feed and stripping compartments were sampled at a fixed time interval, and the concentration was determined by measuring UV absorbance. The wavelengths of maximum absorbance are listed in Table 2. The relationship between concentration and absorbance was calibrated by taking spectra of known concentrations. The diffusion of solutes through the membrane was monitored by periodically removing  $1\text{cm}^3$  samples from both diffusion cells.

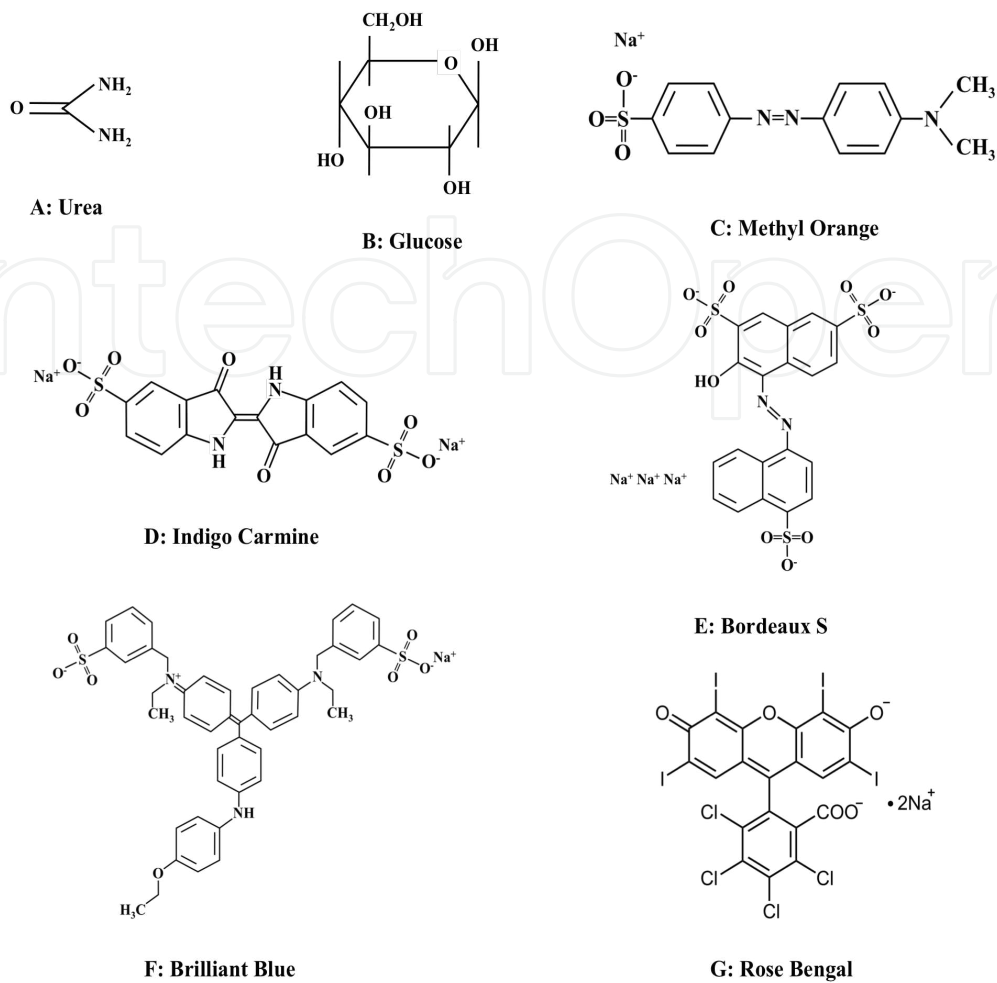


**Figure 9.** Chemical structure of the water-soluble components.

Marker components	Molecular Weight [Da]	Molecular Size [Å]	pH <sup>a</sup>	Structural Formula
Urea	60	6.0	5.4	NH <sub>2</sub> CONH <sub>2</sub>
Glucose	180	8.9	5.8	C <sub>6</sub> H <sub>12</sub> O <sub>6</sub>
Methyl Orange	327	10.6	5.6	C <sub>14</sub> H <sub>14</sub> N <sub>9</sub> O <sub>9</sub> SNa
Indigo Carmine	466	11.9	5.4	C <sub>16</sub> H <sub>8</sub> N <sub>2</sub> Na <sub>2</sub> O <sub>9</sub> S <sub>2</sub>
Bordeaux S	604	13.0	5.9	C <sub>20</sub> H <sub>11</sub> N <sub>2</sub> Na <sub>3</sub> O <sub>10</sub> S <sub>3</sub>
Brilliant Blue	826	14.4	5.5	C <sub>45</sub> H <sub>44</sub> N <sub>3</sub> NaO <sub>7</sub> S <sub>2</sub>
Rose Bengal	1017	15.6	5.8	C <sub>20</sub> H <sub>2</sub> Cl <sub>4</sub> I <sub>4</sub> Na <sub>2</sub> O <sub>5</sub>

<sup>a</sup> Determined from the marker component aqueous solutions of concentration at 1mM.

**Table 2.** The water-soluble components and their molecular size.

## 6.2. Determination of effective diffusion coefficient ( $D_{eff}$ ) in the biopolymer

The concentration of the solution transported through the membrane is required to estimate the mass-transfer characteristics of the membrane. Diffusion is a fundamental phenomenon in several physical and chemical molecular processes, representing the molecular motion of neutral or charged species in solutions [80]. The diffusion coefficient in liquid is an important parameter for understanding the complex processes of mass transfer. Several empirical methods for estimating the diffusion coefficient in aqueous phase consider infinite dilution and are based on molecular-size indicators. Figure 10 presents a schematic of the mass-transfer model. This chapter introduces the following method [81].

$$\text{Wilke \& Chang, } D_w = \frac{1.86 \times 10^{-18} (\phi_B M_w)^{0.5}}{\mu_w v_A^{0.6}} \quad (5)$$

Here,  $D_w$  is the diffusion coefficient of the solute in water [ $\text{m}^2 \text{s}^{-1}$ ],  $\mu_w$  is the viscosity of water [ $\text{Pa s}$ ], and  $\phi_B$  is the association factor for solvent B at the required temperature T [K] (for water,  $\phi_B=2.6$ ).  $M_w$  is the molar mass of water [ $\text{g mol}^{-1}$ ], and  $v_A$  is the molar volume of solute A at the normal boiling point [ $\text{m}^3 \text{mol}^{-1}$ ].

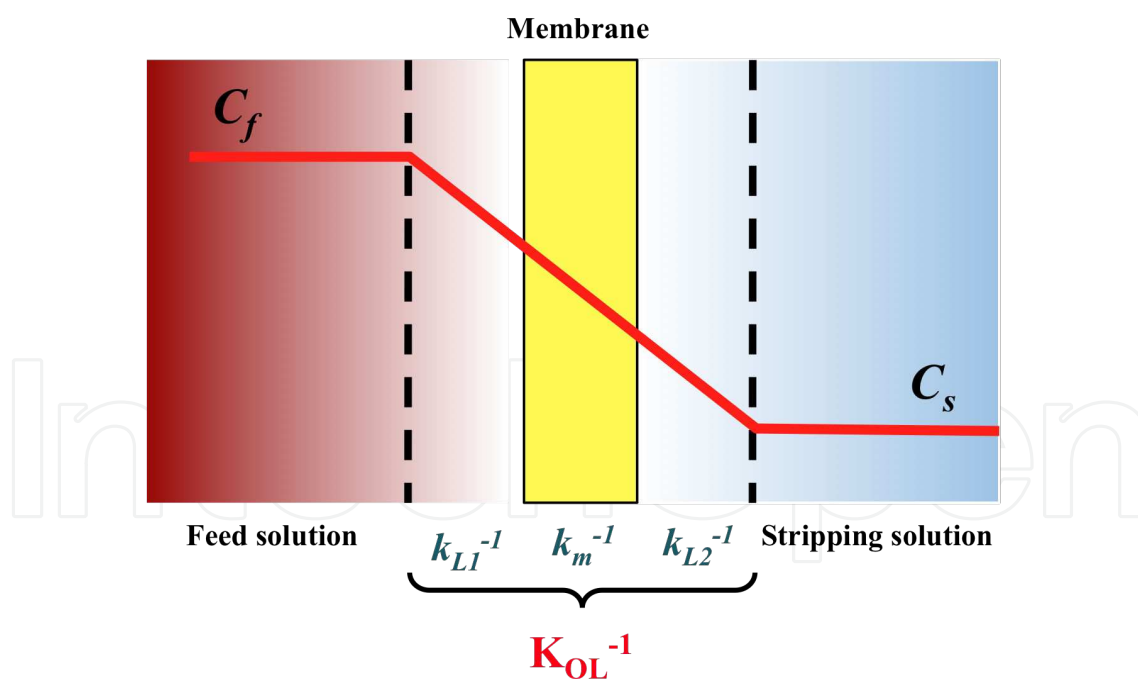


**Figure 10.** The schematic mass transfer model.

The concentrations in the two diffusion cells were uniform, so the mass-transfer flux was so small that the diffusion process can be regarded as in the quasi-steady state. Accordingly, we can use Eqs. (6) and (7) to calculate the effective diffusion coefficients.



$$\ln\left(1 - \frac{2C_s}{C_f}\right) = -2 \frac{A}{V} K_{OL} t \quad (6)$$

$$K_{OL}^{-1} = k_{L1}^{-1} + k_m^{-1} + k_{L2}^{-1} \quad (7)$$

The mass-transfer resistances  $k_{L1}^{-1}$  and  $k_{L2}^{-1}$  in the overall mass transfer resistance  $K_{OL}^{-1}$  can be neglected because of the sufficiently turbulent conditions in the two diffusion cells during the experiment.  $K_{OL}^{-1}$  did not depend on the stirring rate, therefore it directly indicates the membrane mass-transfer coefficient ( $k_m = Deff l^{-1}$ ). The effective diffusion coefficient in the membrane ( $Deff$ ) was evaluated from  $k_m$ . The initial membrane thickness  $l$  in the swollen state was measured with a micrometer.

The mass-transfer characteristics were evaluated from the effective diffusion coefficient estimated by measuring the mass-transfer rate in the composite membrane. Water-soluble components were employed to determine the size of the transfer channel in the membrane. The reference molecular size was from 60 to 1017Da indicating Urea, Glucose, Methyl Orange, Indigo Carmine, Bordeaux S, Brilliant Blue, and Rose Bengal (Table 2). The diffusion coefficient ( $D_w$ ) in the bulk aqueous phase was estimated by Wilke & Chang's correlation (Eq. (5)). The effective diffusion coefficient in the membrane ( $Deff$ ) was lower than  $D_w$  due to diffusion channels in the composite membranes (Fig. 11).

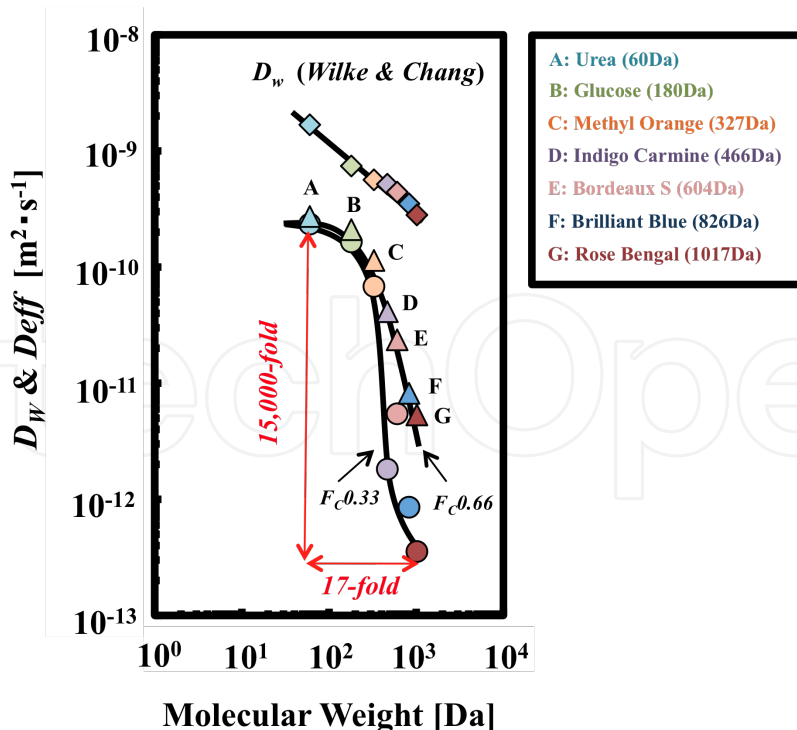


**Figure 11.** Effect of molecular weight on the effective diffusion coefficient of a  $\kappa$ -carrageenan/pullulan composite membrane.

The effective diffusion coefficient in the membrane ( $D_{eff}$ ) changed dramatically by 15,000-fold in molecular weight when molecular weight only changed by 17-fold. The effective diffusion coefficients of the components of lower molecular weight strongly depended on the  $\kappa$ -carrageenan fraction  $F_C$ .  $D_{eff}$  evidently decayed under lower  $F_C$  conditions. The large dependence of  $D_{eff}$  on  $F_C$  suggests that the polymer framework becomes denser with lower  $F_C$ . In addition, there was a steep change of the effective diffusion coefficient between Methyl Orange and Indigo Carmine in each type of composite membrane. The authors therefore speculated that the mass-transfer channel was monodisperse and almost equivalent to the molecular size (11Å) of Methyl Orange.

## 7. Water permeability

In pressure-driven membrane separation processes such as RO and NF, solvent permeability estimation has to consider the series of resistances to fluid flux, including the membrane resistance and the boundary layer proposed, to explain the mass transfer and the hydrodynamic permeability in these processes [82]. The mass transfer inside the membrane in the absence of any osmotic effect using pure solvent (pure water) as feed indicated the moisture sensitivity of polymers. Permeability should be a more reliable indicator [83-84]. Enhancement of water permeability of the filtration membrane reduces the cost of modules used.

Goldstick [85] argued that water permeation flux in membranes follows Darcy's law for hydrodynamic flow through porous media but with swelling-pressure gradients driving the transport. In 1856, Darcy observed that the rate of flow of water through a bed of given thickness could be related to the driving pressure  $\Delta P$  by the simple expression.

$$\frac{1}{A} \cdot \frac{dV}{dt} = J = \frac{\Delta P}{\eta R_m} \quad (8)$$

where  $J$  is the volumetric flux (of volume  $V$  permeating in time  $t$  through cross-section area  $A$ ,  $\text{m}^3/\text{m}^2\text{s}$ ) for the pressure gradient ( $\Delta P$ , Pa) and the viscosity of the fluid ( $\eta$ , Pa·s);  $R_m$  refers to the permeability of the clean porous media. The resistance model is based on Darcy's law, which states that water flux through a membrane is proportional to the pressure gradient across the medium and the permeability of the medium.

If there is no fouling (clean membrane), if feed water is completely free of any solutes, and assuming laminar flow through capillary tubes of radius  $r$ , the Hagen–Poiseuille law was obtained.

$$J = \frac{\varepsilon r^2}{8\eta\tau} \frac{\Delta P}{\Delta x} \quad (9)$$

where

$\varepsilon$  = void fraction of the membrane (void was assumed to be cylindrical pores) ( $n\pi r^2$  /surface area)

$n$  = number of pores

$r$  = pore radius [m]

$\eta$  = viscosity [Pa s]

$\tau$  =tortuosity factor

$\Delta P$  = trans-membrane pressure [Pa]

$\Delta x$  = membrane thicknee [m]

Flux is proportional to porosity, pore size, and trans-membrane pressure.

To study the performance of prepared membranes, pure-water permeability through a  $\kappa$ -carrageenan/pullulan membrane was measured under steady-state conditions. Prior to the experiments, the membranes were immersed in pure water for 12h and then cut into the desired size needed for fixing in a pure water permeability set-up.

The pure-water permeability experiment used a filtration cell with a volume of 200mL and effective filtration area of 21cm<sup>2</sup>. A magnetic stirring bar was installed on the membrane upper surfaces. The filtration cell was employed for constant-flux, constant-pressure filtration. For operation in the constant-flux mode, a nitrogenous gas pump was connected to the inlet of the filtration cell and pumped the permeation water from the outlet. A pressure transducer was installed between the filtration cell and the pump in order to monitor the variation in applied pressure during filtration. The weight of the filtration water was logged by an electronic balance. The schematic of the module and set-up is presented in Fig. 12. In this chapter, the pure-water permeability was measured at different pressures and using Eq. 10.

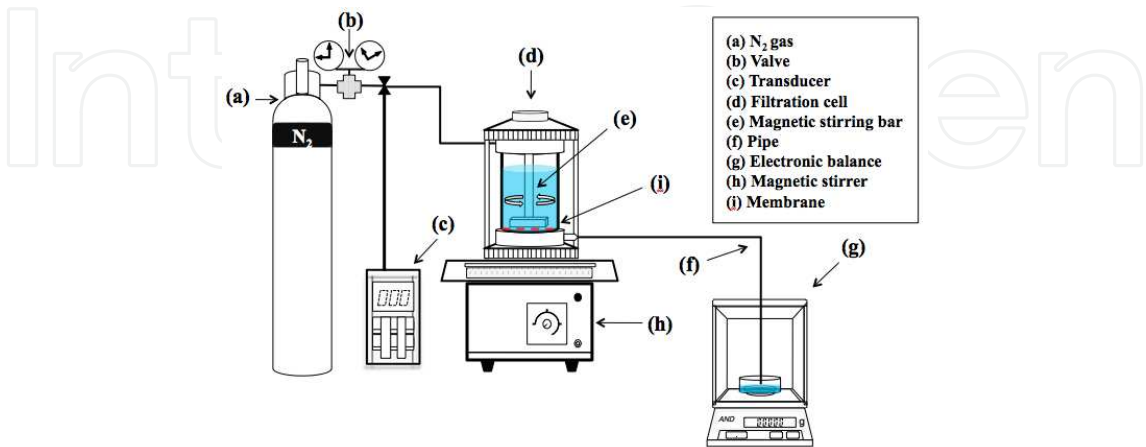


**Figure 12.** Schematic diagram of filtration cell used to measure steady pure-water permeability through the membranes.

$$J_V = \frac{V_P}{A\Delta t} \quad (10)$$

Here,  $J_V$  is the water flux [ $\text{m}^3 \text{m}^{-2} \text{s}^{-1}$ ],  $V_p$  is the volumetric amount of permeated water [ $\text{m}^3$ ],  $A$  is the membrane area [ $\text{m}^2$ ], and  $\Delta t$  is the sampling time [s].

The pure-water flux was measured as a function of applied pressure to investigate the stability and hydraulic properties of biopolymer membranes. In Fig. 13, the water flux and content increased linearly with increasing  $F_C$ . The result agreed with the general trend of water permeation in a hydrophilic membrane: higher water content induced higher water flux.

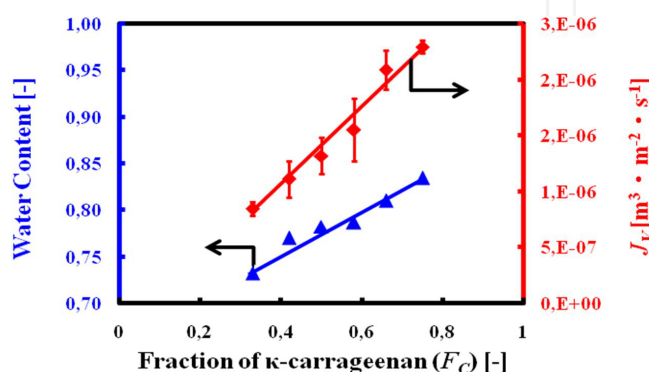


**Figure 13.** Change of the water flux (150KPa, 298K) and the water content of the membrane with regulated  $F_C$  values.

### 7.1. Obtaining the selectivity curve and molecular weight cutoff

The selectivity of a membrane is usually represented by its molecular weight cutoff [86], defined as the minimum molar mass of a test solute that is 90% retained (or 95% depending on the manufacturer) by the membrane. It is thus determined experimentally from a plot of the variation of the retention rate for tracer molecules according to their molar mass (i.e., from the selectivity (or sieving) curve) (Fig. 14).

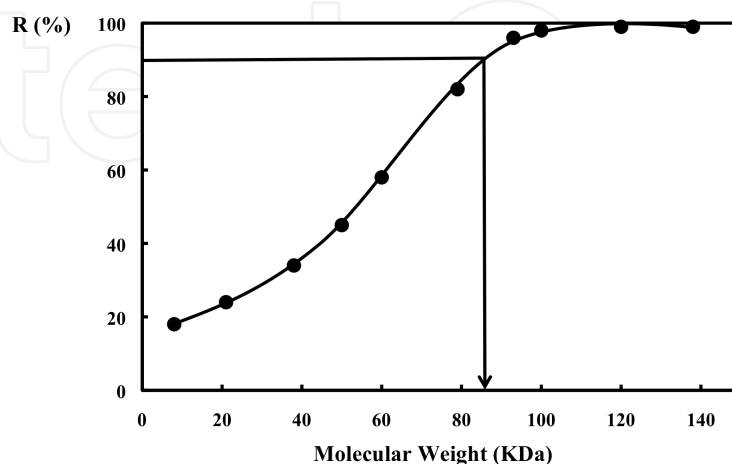


**Figure 14.** Example of a selectivity curve. The molecular weight cutoff, i.e., the molecular weight of a molecule rejected at 90% by the membrane is 83 kDa.

To determine a cutoff threshold, an intrinsic characteristic of the biopolymer membrane only, it is essential that the operating conditions (trans-membrane pressure, tangential circulation speed, etc.) should not affect the retention data. The rejection used for molecular weight cutoff evaluation was defined as follows.

$$R = \frac{\text{FeedConc.} - \text{PermeateConc.}}{\text{FeedConc.}} \quad (11)$$

Figure 15 presents the effect of  $F_c$  on the molecular weight cutoff of the  $\kappa$ -carrageenan/pullulan membranes. The molecular weight cutoff and the flux of  $\kappa$ -carrageenan/pullulan membranes increased with increasing  $F_c$  (Fig. 15). The molecular cutoff of  $F_c 0.33$  ( $F_c 0.66$ ) membrane was 327Da (466Da). The retention for high-molecular-weight tracers above 604Da was 96 to 98%.

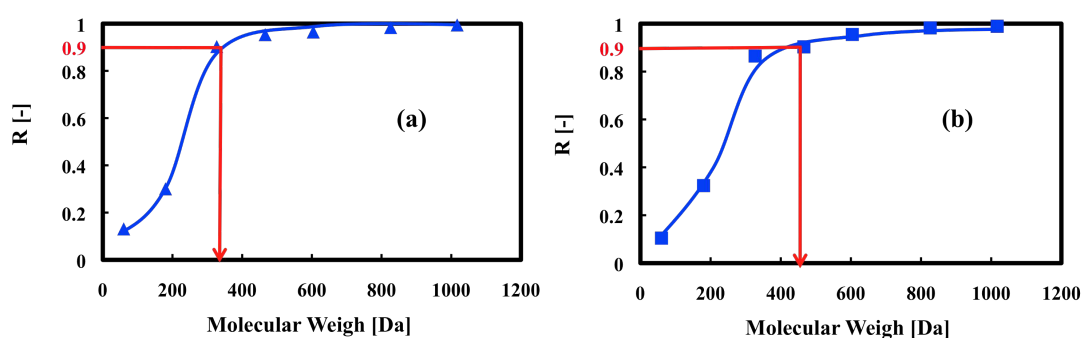


**Figure 15.** The selective curve of  $\kappa$ -carrageenan/pullulan membrane for dye molecules. (a):  $F_c 0.33$  membrane, (b):  $F_c 0.66$  membrane.

## 8. Conclusions

There are increasing reports on the physicochemical behavior of well-characterized biopolymer systems based on the fundamentals of gelation, and component interactions in the bulk and at interfaces. It appears, however, that a gap has emerged between the recent advances in fundamental knowledge and the direct application to products with a growing need for scientific input. As can be seen from the above, biopolymers are now one of the most explored potential materials for membrane-separation technology, but there is much experimental and theoretical work left to complete. An analysis of the structure–property relationships provides much information on the effects of side groups, structure, and stiffness of the main chains that can be used in directed search for advanced membrane materials of other classes. Much more interesting results have been obtained for composite and modified biopolymers. Here, significantly fewer structures have been examined, so much is yet to be done.

Biopolymer  $\kappa$ -carrageenan/pullulan composite membrane was successfully prepared by the casting method. It has sufficient mechanical strength for practical use and excellent mass-transfer characteristics, especially for molecular-size screening. The relationship between

mass-transfer characteristics and the mass fraction of  $\kappa$ -carrageenan in the composite membrane was formulated based on mass-transfer flux and pure-water flux experiments. The results provided a novel and simple method of preparing membranes and mass-transfer channels based on molecular-size indicators, and suggested that different  $F_c$  values significantly affect the mass-transfer permeability. The water permeation flux as a function of applied pressure provided valuable technical information for investigating the stability and hydraulic properties of the composite membranes. It was concluded that  $\kappa$ -carrageenan/pullulan composite membranes with a cross-linked hydrophilic structure exhibited high selectivity and high water flux. Thus, mass-transfer investigations are very useful and informative for studying and analyzing composite membranes.

## Acknowledgements

This work was supported by research funding grants provided by the Iijima Memorial Foundation for the Promotion of Food Science and Technology. The authors sincerely thank Dr. Kei Tao of Nihon University, who provided technical assistance on SEM photography.

## Author details

Peng Wu and Masanao Imai\*

\*Address all correspondence to: [XLT05104@nifty.com](mailto:XLT05104@nifty.com)

Course in Bioresource Utilization Sciences, Graduate School of Bioresource Sciences, Nihon University, Japan

## References

- [1] Krishna, R. K. S. V., Vijaya, B., Naidu, K., Subha, M. C. S., Sairam, M., Mallikarjuna, N. N., & Aminabavi, T. M. (2006). Novel carbohydrate polymeric blend membranes in pervaporation dehydration of acetic acid. *Carbohydrate Polymer*, 66, 345-351.
- [2] Stanek, L. G., Heilmann, S. M., & Gleason, W. B. (2006). Preparation and copolymerization of a novel carbohydrate containing monomer. *Carbohydrate Polymer*, 65, 552-556.
- [3] Lee, K. P., Arnot, T. C., & Mattia, D. (2011). A review of reverse osmosis membrane materials for desalination-Development to date and future potential. *Journal of Membrane Science*, 370, 1-22.
- [4] Catherine, C. (2009). A review of membrane processes and renewable energies for desalination. *Desalination*, 245, 214-231.



- [5] Guessasma, S., Hamdi, A., & Lourdin, D. (2009). Linear modeling of biopolymer systems and related mechanical properties. *Carbohydrate Polymer*, 76, 381-388.
- [6] Imeson, A. (2009). Food Stabilisers, Thickeners and Gelling Agents. Wiley-Blackwell, 343, 10.1002/9781444314724.
- [7] Kumar, A., Srivastava, A., Galaev, I. Y., & Mattiasson, B. (2007). Smart polymer: Physical forms and bioengineering applications. *Prog. Polym. Sci.*, 32, 1205-1237.
- [8] Clark, A. H. (1996). Biopolymer gels. *Current Opinion in Colloid & Interface Science*, 1, 712-717.
- [9] McCray, S. B., Vilker, V. L., & Nobe, K. (1991). Reverse osmosis cellulose acetate membranes. I. Rate of hydrolysis. *Journal of Membrane Science*, 59, 305-316.
- [10] Rinaudo, M. (2006). Chitin and chitosan: Properties and applications. *Prog. Polym. Sci.*, 31, 603-632.
- [11] Pillai, C. K. S., Paul, W., & Sharma, C. P. (2009). Chitin and chitosan polymers: Chemistry, solubility and fiber formation. *Progress in polymer Science*, 34, 641-678.
- [12] Lee, Y. M., & Shin, E. M. (1991). Pervaporation separation of water-ethanol through modified chitosan membranes. IV. Phosphorylated chitosan membranes. *Journal of Membrane Science*, 64, 145-152.
- [13] Won, W., Feng, X. S., & Lawless, D. (2002). Pervaporation with chitosan membranes: separation of dimethyl carbonate/methanol/water mixtures. *Journal of Membrane Science*, 209, 493-508.
- [14] Devi, D. A., Smitha, B., Sridhar, S., & Aminabhavi, T. M. (2005). Pervaporation separation of isopropanol/water mixtures through crosslinked chitosan membranes. *Journal of Membrane Science*, 262, 91-99.
- [15] Huang, X. J., Ge, D., & Xu, Z. K. (2007). Preparation and characterization of stable chitosan nanofibrous membrane for lipase immobilization. *European Polymer Journal*, 43, 3710-3718.
- [16] Beppu, M. M., Vieira, R. S., Aimoli, C. G., & Santana, C. C. (2007). Crosslinking of chitosan membranes using glutaraldehyde: Effect on ion permeability and water absorption. *Journal of Membrane Science*, 301, 126-130.
- [17] Zeng, X. F., & Ruckenstein, E. (1998). Cross-linked macroporous chitosan anion-exchange membranes for protein separations. *Journal of Membrane Science*, 148, 195-205.
- [18] Takahashi, T., Imai, M., Suzuki, I., & Sawai, J. (2008). Growth inhibitory effect on bacteria of chitosan membranes regulated with deacetylation degree. *Biochemical Engineering Journal*, 40, 485-491.
- [19] Takahashi, T., Imai, M., & Suzuki, I. (2007). Water permeability of chitosan membrane involved in deacetylation degree control. *Biochemical Engineering Journal*, 36, 43-48.

- [20] Kashima, K., Imai, M., & Suzuki, I. (2010). Superior molecular size screening and mass-transfer characterization of calcium alginate membrane. *Desalination and water treatment*, 17, 143-159.
- [21] Kashima, K., & Imai, M. (2011). Dominant impact of the  $\alpha$ -L-guluronic acid chain on regulation of the mass transfer character of calcium alginate membranes. *Desalination and water treatment*, 134, 257-265.
- [22] El Gamal, A. A. (2010). Biological importance of marine algae. *Saudi Pharmaceutical Journal*, 18, 1-25.
- [23] Rasmussen, R. S., & Morrissey, M. T. (2007). Marine biotechnology for production of food ingredients. *Advances in Food and Nutrition Research*, 52, 237-292.
- [24] Millane, R. P., Chandrasekaran, R., & Arnott, S. (1988). The molecular structure of kappa-carrageenan and comparison with iota-carrageenan. *Carbohydrate Research*, 183, 1-17.
- [25] Dea, I. C. M., Mckinnon, A. A., & Rees, D. A. (1972). Tertiary and Quaternary Structure in Aqueous Polysaccharide Systems which Model Cell Wall Cohesion: Reversible Changes in Conformation and Association of Agarose, Carrageenan and Galactomannans. *Journal of Molecular Biology*, 68, 153-172.
- [26] Bixler, H. J., Johndro, K., & Falshaw, R. (2001). Kappa-2 carrageenan: structure and performance of commercial extracts II. Performance in two simulated dairy applications. *Food Hydrocolloids*, 15, 619-630.
- [27] Falshaw, R., Bixler, H. J., & Johndro, K. (2001). Structure and performance of commercial kappa-2 carrageenan extracts I. Structure analysis. *Food Hydrocolloids*, 15, 441-452.
- [28] Ekstrom, A. G., & Kuivinen, J. (1983). Molecular weight distribution and hydrolysis behaviour of carrageenans. *Carbohydrate Research*, 116, 89-94.
- [29] El Gamal, A. A. (2010). Biological importance of marine algae. *Saudi Pharmaceutical Journal*, 18, 1-25.
- [30] Mangione, M. R., Giacomazza, D., Bulone, D., Martorana, V., Cavallaro, G., & San Biagio, P. L. (2005).  $K^+$  and  $Na^+$  effects on the gelation properties of k-Carrageenan. *Biophysical Chemistry*, 113, 129-135.
- [31] Leathers, T. D. (2003). Biotechnological production and applications of pullulan. *Appl Microbiol Biotechnol.*, 62, 468-473.
- [32] Ueda, S., Fujita, K., Komatsu, K., & Nakashima, Z. (1963). Polysaccharide produced by the genus Pullularia I. Production of polysaccharide by growing cells. *Applied Microbiology*, 11, 211-215.
- [33] Singh, R. S., Saini, G. K., & Kennedy, J. F. (2008). Pullulan: Microbial sources, production and applications. *Carbohydrate Polymers*, 73, 515-531.

- [34] Xiao, Q., Lim, L. T., & Tong, Q. (2011). Properties of pullulan-based blend film as affected by alginate content and relative humidity. *Carbohydrate Polymers*, 87, 227-234.
- [35] Shih, F. F., Daigle, K. W., & Champagne, E. T. (2011). Effect of rice wax on water vapour permeability and sorption properties of edible pullulan films. *Food Chemistry*, 127, 118-121.
- [36] Lazaridou, A., Biliaderis, C. G., & Kontogiorgos, V. (2003). Molecular weight effects on solution rheology of pullulan and mechanical properties of its films. *Carbohydrate Polymers*, 52, 151-166.
- [37] Trinetta, V., Cutter, C. N., & Floros, J. D. (2011). Effects of ingredient composite on optical and mechanical properties of pullulan film for food-packaging applications. *LWT- Food Science and Technology*, 44, 2296-2301.
- [38] Ulbricht, M. (2006). Advanced functional polymer membranes. *Polymer*, 47, 2217-2262.
- [39] Lebrun, L., Blanco, J. F., & Metayer, M. (2005). Preparation of ion-exchange membranes using pullulan as polymer matrix. *Carbohydrate Polymers*, 61, 1-4.
- [40] Datta, S., Mody, K., Gopalsamy, G., & Jha, B. (2011). Novel application of  $\kappa$ -carrageenan: As a gelling agent in microbiological media to study biodiversity of extreme alkaliphiles. 85, 465-468.
- [41] Wu, P., & Imai, M. (2011). Food polymer pullulan- $\kappa$ -carrageenan composite membrane performed smart function both on mass transfer and molecular size recognition. *Desalination and Water Treatment*, 34, 239-245.
- [42] Sairam, M., Sereewatthanawut, E., Li, K., Bismarck, A., & Livingston, A. G. (2011). Method for the preparation of cellulose acetate flat sheet composite membranes for forward osmosis-Desalination using  $\text{MgSO}_4$  draw solution. *Desalination*, 273, 299-307.
- [43] Miao, J., Chen, G., Gao, C., & Dong, S. X. (2008). Preparation and characterization of N,O-carboxymethyl chitosan/Polysulfone composite nanofiltration membrane cross-linked with epichlorohydrin. *Desalination*, 233, 147-156.
- [44] Peeva, P. D., Million, N., & Ulbricht, M. (2012). Factors affecting the sieving behavior of anti-fouling thin-layer cross-linked hydrogel polyethersulfone composite ultrafiltration membranes. *Journal of Membrane Science*, 390-391, 99-112.
- [45] Elimelech, M., Zhu, X. H., Childress, A. E., & Hong, C. S. (1997). Role of membrane surface morphology in colloidal fouling of cellulose acetate and composite aromatic polyamide reverse osmosis membranes. *Journal of Membrane Science*, 127, 101-109.
- [46] Zio, A. D., Prisciandaro, M., & Barda, D. (2005). Disinfection of surface waters with UF membranes. *Desalination*, 179, 297-305.
- [47] Singh, G., Rana, D., Matsuura, T., Ramakrishna, S., Narbaitz, R. M., & Tabe, S. (2010). Removal of disinfection byproducts from water by carbonized electrospun nanofibrous membranes. *Separation and Purification Technology*, 74, 202-212.

- [48] Lameloise, M., Matinier, H., & Fargues, C. (2009). Concentration and purification of malate ion from a beverage industry waste water using electrodialysis with homopolar membranes. *Journal of Membrane Science*, 343, 73-81.
- [49] Yushina, Y., & Hasegawa, J. (1994). Process performance comparison of membrane introduced anaerobic digestion using food industry waste water. *Desalination*, 98, 413-421.
- [50] Blocher, C., Noronha, M., Funfrocken, L., Dorda, J., Mavrov, V., Janke, H. D., & Chmiel, H. (2002). Recycling of spent process water in the food industry by an integrated process of biological treatment and membrane separation. *Desalination*, 144, 143-150.
- [51] Alp, B., Mutltu, S., & Mutlu, M. (2000). Glow-discharge-treated cellulose acetate (CA) membrane for a high linearity single-layer glucose electrode in the food industry. *Food Research International*, 33, 107-112.
- [52] Kabay, N., Bryjak, M., Schlosser, S., Kitis, M., Avlonitis, S., Matejka, Z., Al-Mutaz, I., & Yuksel, M. (2008). Adsorption-membrane filtration (AMF) hybrid process for boron removal from seawater: an overview. *Desalination*, 223, 38-48.
- [53] Redondo, J., Busch, M., & Witte, J. D. (2003). Boron removal from seawater using FILMTECTM high rejection SWRO membranes. *Desalination*, 156, 229-238.
- [54] Hu, J. H., Song, L. F., Ong, S. L., Phua, E. T., & Ng, W. J. (2005). Biofiltration pretreatment for reverse osmosis (RO) membrane in a water reclamation system. *Chemosphere*, 59, 127-133.
- [55] Alvarez-Hornos, F. J., Volckaert, D., Heynderickx, P. M., & Langenhove, H. V. (2011). Performance of a composite membrane bioreactor for the removal of ethyl acetate from waste air. *Bioresource Technology*, 102, 8893-8898.
- [56] Zheng, X., & Liu, J. (2006). Dyeing and printing wastewater treatment using a membrane bioreactor with a gravity drain. *Desalination*, 190, 277-286.
- [57] Su, M., Teoh, M. M., Wang, K. Y., Su, J. C., & Chung, T. S. (2010). Effect of inner-layer thermal conductivity on flux enhancement of dual-layer hollow fiber membranes in direct contact membrane distillation. *Journal of Membrane Science*, 364, 278-289.
- [58] Shah, B. G., Shahi, V. K., Thampy, S. K., Rangarajan, R., & Ghosh, P. K. (2009). Comparative studies on performance of interpolymer and heterogeneous ion-exchange membranes for water desalination by electrodialysis. *Desalination*, 172, 257-265.
- [59] Misdan, N., Lau, W. J., & Ismail, A. F. (2012). Seawater Reverse Osmosis (SWRO) desalination by thin-film composite membrane-Current development, challenges and future prospects. *Desalination*, 287, 228-237.
- [60] Maguire-Boyle, S. J., & Barron, A. R. (2011). A new functionalization strategy for oil/water separation membranes. *Journal of Membrane Science*, 382, 107-115.

- [61] Steward, P. A., Hearn, J., & Wilkinson, M. C. (2000). An overview of polymer latex film formation and properties. *Advances in Colloid and Interface Science*, 86, 195-267.
- [62] Tong, Q., Xiao, Q., & Lim, L. T. (2008). Preparation and properties of pullulan-alginate-carboxymethylcellulose blend films. *Food Research International*, 41, 1007-1014.
- [63] Martelli, S. M., Moore, G. R. P., & Laurindo, J. B. (2006). Mechanical Properties, Water Vapor Permeability and Water Affinity of Feather Keratin Films Plasticized with Sorbitol. *J. Polym. Environ.*, 14, 215-222.
- [64] Rao, P. S., Smitha, B. S., Sridhar, S., & Krishnaiah, A. (2006). Preparation and performance of poly(vinyl alcohol)/polyethyleneimine blend membranes for the dehydration of 1,4-dioxane by pervaporation: Comparison with glutaraldehyde cross-linked membranes. *Separation and Purification Technology*, 48, 244-254.
- [65] Takahashi, T., Imai, M., & Suzuki, I. (2008). Cellular structure in an N-acetyl-chitosan membrane regulate water permeability. *Biochemical Engineering Journal*, 42, 20-27.
- [66] McCray, S. B., Vilker, V. L., & Nobe, K. (1991). Reverse osmosis cellulose acetate membranes. I. Rate of hydrolysis. *Journal of Membrane Science*, 59, 305-316.
- [67] Vasileva, N., & Godjevargova, T. (2004). Study on the behaviour of glucose oxidase immobilized on microfiltration polyamide membrane. *Journal of Membrane Science*, 239, 157-161.
- [68] Villegas, M., Vidaurre, E. F., Habert, A. C., & Gottifredi, J. C. (2011). Sorption and pervaporation with poly(3-hydroxybutyrate) membranes: methanol/methyl tert-butyl ether mixtures. *Journal of Membrane Science*, 367, 103-109.
- [69] Matsuoka, Y., Kanda, N., Lee, Y. M., & Higuchi, A. (2006). Chiral separation of phenylalanine in ultrafiltration through DNA-immobilized chitosan membranes. *Journal of Membrane Science*, 280, 116-123.
- [70] Papageorgiou, S. K., Katsaros, F. K., Favvas, E. P., Romanos, G. E., Athanasekou, C. P., Beltsios, K. G., Tziaila, O. I., & Falaras, P. (2012). Alginate fibers as photocatalyst immobilizing agents applied in hybrid photocatalytic/ultrafiltration water treatment processes. *Water Research*, 46, 1858-1872.
- [71] Miao, J., Chen, G. H., & Gao, C. J. (2005). A novel kind of amphoteric composite nanofiltration membrane prepared from sulfated chitosan (SCS). *Desalination*, 181, 173-183.
- [72] Li, X. L., Zhu, L. P., Zhu, B. K., & Xu, Y. Y. (2011). High-flux and anti-fouling cellulose nanofiltration membranes prepared via phase inversion with ionic liquid as solvent. *Separation and Purification Technology*, 83, 66-73.
- [73] Wu, J., & Yuan, Q. (2002). Gas permeability of a novel cellulose membrane. *Journal of Membrane Science*, 204, 185-194.



- [74] Xiao, S., Feng, X. S., & Huang, R. Y. M. (2007). Trimesoyl chloride crosslinked chitosan membranes for CO<sub>2</sub>/N<sub>2</sub> separation and pervaporation dehydration of isopropanol. *Journal of Membrane Science*, 306, 36-46.
- [75] Feil, H., Bae, Y. H., Feijen, J., & Kim, S. W. (1991). Molecular separation by thermosensitive hydrogel membranes. *Journal of Membrane Science*, 64, 283-294.
- [76] Peppas, N. A., & Reinhart, C. (1983). Solute Diffusion in Swollen Membranes. Part I. A New Theory. *Journal of Membrane Science*, 15, 275-287.
- [77] Baltus, R. E. (1997). Characterization of the pore area distribution in porous membranes using transport measurements. *Journal of Membrane Science*, 123, 165-184.
- [78] Krajewska, B., & Olech, A. (1996). Pore structure of gel chitosan membranes. I. Solute diffusion measurements. *Polymer Gels and Networks*, 4, 33-43.
- [79] Neogi, P. (1996). Diffusion in Polymer. Marcel Dekker, 309.
- [80] Chen, C. X., Han, B. B., Li, J. D., Shang, T. G., & Jiang, W. J. (2001). A new model on the diffusion of small molecule penetrants in dense polymer membranes. *Journal of Membrane Science*, 187, 109-118.
- [81] Miyabe, K., & Isogai, R. (2011). Estimation of molecular diffusivity in liquid phase systems by the Wilke-Chang equation. *Journal of Chromatography A*, 1218, 6639-6645.
- [82] Mehdizadeh, H., Molaiee-Nejad, K., & Chong, Y. C. (2005). Modeling of mass transport of aqueous solutions of multi-solute organics through reverse osmosis membranes in case of solute-membrane affinity Part 1. Model development and simulation. *Journal of Membrane Science*, 267, 27-40.
- [83] Yaroshchuk, A. E. (1995). Solution-diffusion-imperfection model revised. *Journal of Membrane Science*, 101, 83-87.
- [84] Yaroshchuk, A. E. (1995). The role of imperfections in the solute transfer in nanofiltration. *Journal of Membrane Science*, 239, 9-15.
- [85] Fatt, I., & Goldstick, T. K. (1965). Dynamics of water transport in swelling membranes. *J. Colloid Sci.*, 20, 962-989.
- [86] Jonsson, G. (1985). Molecular weight cut-off for ultrafiltration membranes of varying pore size. *Desalination*, 53, 3-10.



